Available online at www.sciencedirect.com
ScienceDirect
JOURNAL OF COMPUTATIONAL AND APPLIED MATHEMATICS
Journal of Computational and Applied Mathematics 223 (2009) 86–96
www.elsevier.com/locate/cam

G^1 interpolation with a single Cornu spiral segment

D.J. Walton[a,*], D.S. Meek[b]

[a] Department of Computer Science and St. Paul's College, University of Manitoba, 70 Dysart Road, Winnipeg, Manitoba R3T 2M6, Canada
[b] Department of Computer Science, University of Manitoba, Winnipeg, Manitoba R3T 2N2, Canada

Received 15 August 2007; received in revised form 14 December 2007

Abstract

Cornu spiral segments are used in applications such as the geometric design of highways and railways, robot path planning, and shape completion. For some applications, e.g. shape completion in computer vision, it is important to use a single visually pleasing curve segment to smoothly fill a gap, even though the gap may not be filled in a curvature continuous manner. An improved method for doing so using a Cornu spiral segment is discussed. The method is generally suitable for any application where it is required to smoothly fit a curve between two given points when the corresponding tangent directions, but not the curvatures, are also given or known.

MSC: 65D17; 68U07 (CAD)

Keywords: Cornu spiral; Clothoid; Euler spiral; G^1 interpolation

1. Introduction

Spiral segments are used in the design of highway and railway routes, trajectories of mobile robots and other similar applications. A special spiral, known as Euler's spiral, Cornu's spiral, or the clothoid, is popular for such applications mainly because its curvature is a linear function of its arclength [2,3,5,7,15].

Fitting a planar curve between two given points such that it matches the unit tangent vectors at the points, is called two point G^1 Hermite interpolation. If given curvatures at the two points are also matched, then it is called two point G^2 Hermite interpolation.

A Cornu spiral segment has six degrees of freedom which are insufficient for G^2 Hermite interpolation. Several techniques have thus been developed that use a pair of Cornu spiral segments to provide more degrees of freedom. These include methods for blending or transition curves which are suitable for applications such as the geometric design of highway and railway routes, or the design of trajectories for mobile robots [11,17–19]. For such applications the positions of the points are not fixed; the points are allowed to move on the circumference of a circle, or along a straight line. There are also methods which use a circular arc in conjunction with a pair of Cornu spiral segments for G^2 Hermite interpolation where the points are fixed [12].

* Corresponding author. Tel.: +1 204 474 8679; fax: +1 204 474 7620.
E-mail addresses: walton@cs.umanitoba.ca (D.J. Walton), dmeek@cc.umanitoba.ca (D.S. Meek).

0377-0427/$ - see front matter
doi:10.1016/j.cam.2007.12.022

For some applications certain properties of segments of special curves are more desirable than a G^2 match, or the cost-effectiveness of a G^1 match is preferable. Two such curves are the Pythagorean Hodograph (PH) curve and the Cornu spiral. In [4] a shape-preserving G^2 PH quintic spline is constructed by applying Newton–Raphson iterations to a system of non-linear equations. However, the same article also introduces a simpler shape-preserving G^1 PH quintic spline which can be constructed locally.

Kimia et al. [8] discuss details of the shape completion problem as an application to computer vision, and also mention other applications, including computerised typography. They formulate the problem as:

"Given a pair of points with associated unit tangent vectors, find the most 'pleasing' curve which passes through both points at their respective tangents."

With references to Knuth [9] and Ullman [16], they list the following properties of the most 'pleasing' curve: invariance under translation, rotation and scaling; symmetry; extensibility; locality; smoothness; and roundedness. Their analyses and additional references within [8] lead them to the conclusion that the most 'pleasing' curve is the Cornu (a.k.a. Euler) spiral. The extensibility requirement rules out using a pair of spirals, so G^1 interpolation with a single Cornu spiral segment is proposed.

To solve this problem, Kimia, et al. [8] formulate it mathematically as a system of two non-linear equations in two unknown variables. The system, as formulated, has no direct analytic solution, so they use a gradient descent based numerical optimization technique to obtain a Cornu spiral segment that best matches the given G^1 Hermite data. This approach has the following disadvantages.

- It is not clear whether a solution to the system of equations actually exists and is found, or whether the optimization finds a Cornu spiral segment which is an approximation to the desired curve segment.
- The convergence of the optimization procedure depends on using good starting values for the unknown variables.
- In order to find good starting values, a pre-processing phase is introduced. In this phase the problem is reformulated as a biarc fitting problem which is solved prior to applying the numerical optimization.
- A biarc has seven degrees of freedom, so the biarc which matches given G^1 Hermite data is not unique. This dilemma is resolved by constraining the biarc so that its total squared curvature is minimised.

The purpose of this article is to propose a method for G^1 interpolation with a single Cornu spiral segment which does not suffer from the above disadvantages. This new method considers the C- and S-shaped cases separately. For each case a single non-linear equation in one unknown is derived. Furthermore, for each case, an interval in which the solution occurs, is provided. The solution can be found by a bracketting technique which is guaranteed to provide the solution, or by a combination of bracketting with the Newton–Raphson method for improved performance.

The proposed method is suitable for any given non-degenerate G^1 Hermite data. A circle is actually a special case of the Cornu spiral; it is the limiting case as the arclength of the spiral tends to infinity. Because of precision limitations in a computer, it is advisable to check for "near circularity" at some point in the algorithm and fit a circular arc rather than computing the corresponding Cornu spiral segment, as explained in Section 2.1 below.

It will be shown that the problem is naturally partitioned into three mutually exclusive cases, namely

- a C-shaped case (the beginning and ending tangent vectors point in directions which are on opposite sides of the chord joining the beginning and ending points),
- an S-shaped case where the beginning and ending tangent vectors point in directions which are on opposite sides of the chord joining the beginning and ending points, and
- an S-shaped case where the beginning and ending tangent vectors point in directions which are on the same side of the chord joining the beginning and ending points.

The remainder of this paper is organised as follows. The next section establishes the notation and conventions used; it is followed by a section with background information on the Cornu spiral. The C- and S-shaped cases are then discussed in two separate sections, followed by a section of examples and a section with concluding remarks.

2. Notation and conventions

The usual Cartesian coordinate system with x- and y-axes is presumed. Positive angles are measured counter-clockwise. Boldface is used for points and vectors. Points and vectors may also be indicated using the ordered pair notation, e.g. (x, y). In particular, the components of a vector $\mathbf{V}$ may be denoted as (V_x, V_y). The norm or length of a vector $\mathbf{V}$ is denoted as $\|\mathbf{V}\|$. The derivative of a function (scalar or vector valued), is denoted with a prime, e.g. $X'(t)$ or $\mathbf{Q}'(t)$. A planar parametric curve is defined by the set of points $\mathbf{Q}(t) = (X(t), Y(t))$ for real t.

Define the rotation matrix

$$R(\varphi) = \begin{pmatrix} \cos\varphi & \sin\varphi \\ -\sin\varphi & \cos\varphi \end{pmatrix}.$$

It rotates a row vector counter-clockwise by an angle of φ.

2.1. G^1 Hermite interpolation

Given two distinct points $\mathbf{P}_1, \mathbf{P}_2$ with corresponding unit tangent vectors $\mathbf{T}_1, \mathbf{T}_2$ respectively where $\mathbf{T}_1, \mathbf{T}_2$, and the line segment joining $\mathbf{P}_1$ to $\mathbf{P}_2$, are not all parallel. It is desirable to find a segment of the Cornu spiral which joins $\mathbf{P}_1$ to $\mathbf{P}_2$ such that its unit tangent vectors at those points match $\mathbf{T}_1$ and $\mathbf{T}_2$ respectively. Let $\mathbf{D} = \mathbf{P}_2 - \mathbf{P}_1$, ϕ_1 the angle from $\mathbf{T}_1$ to $\mathbf{D}$, and ϕ_2 the angle from $\mathbf{D}$ to $\mathbf{T}_2$. Assume, without loss of generality, that

- $|\phi_1| \neq |\phi_2|$
- $\mathbf{P}_1$ and $\mathbf{P}_2$ are labelled such that $|\phi_1| < |\phi_2|$.
- The data are (or have been reflected about $\mathbf{D}$ if necessary) such that $0 < \phi_2 < \pi$.

These assumptions avoid the following degenerate and ambiguous cases.

- $\phi_1 = \phi_2 = 0$: This is a straight line segment which joins $\mathbf{P}_1$ to $\mathbf{P}_2$.
- $\phi_1 = \phi_2 \neq 0$: This is a circular arc of radius $r = \frac{1}{2}\|\mathbf{D}\|/\sin\phi_1$, centred at $\mathbf{P}_1 + r\mathbf{T}_1 R(\frac{1}{2}\pi)$
- $\phi_1 = \pm\pi, \phi_2 = \pm\pi$ or $\phi_1 = \pm\pi, \phi_2 = 0$ or $\phi_1 = 0, \phi_2 = \pm\pi$: Two Cornu spiral segments satisfy each of these sets of data; they lie on opposite sides of $\mathbf{D}$.

The ordering also ensures that $\phi_1 + \phi_2 > 0$

3. Background

The Cornu spiral has a single inflection point. A Cornu spiral whose inflection point occurs at $\mathbf{P}_0$ with a unit tangent vector of $\mathbf{T}_0$ at $\mathbf{P}_0$, is defined in terms of the Fresnel integrals as [19]

$$\mathbf{Q}(\theta) = \begin{cases} \mathbf{P}_0 + aC(\theta)\mathbf{T}_0 + aS(\theta)\mathbf{N}_0, & \theta \geq 0, \\ \mathbf{P}_0 - aC(-\theta)\mathbf{T}_0 - aS(-\theta)\mathbf{N}_0, & \theta < 0, \end{cases} \tag{1}$$

where $\mathbf{N}_0 = \mathbf{T}_0 R(\frac{1}{2}\pi)$, the scaling factor a is positive, θ is the tangent angle deviation from $\mathbf{T}_0$ for $\theta \geq 0$, $-\theta$ is the tangent angle deviation from $\mathbf{T}_0$ for $\theta < 0$ and the Fresnel integrals are [1]

$$C(\theta) = \frac{1}{\sqrt{2\pi}} \int_0^\theta \frac{\cos u}{\sqrt{u}} \mathrm{d}u, \quad S(\theta) = \frac{1}{\sqrt{2\pi}} \int_0^\theta \frac{\sin u}{\sqrt{u}} \mathrm{d}u. \tag{2}$$

The following theorem provides a necessary condition for the curve to which a chord is drawn, to be part of a Cornu spiral with positive curvature.

Theorem 1. *Let $\mathbf{D} = \mathbf{Q}(\theta+\delta) - \mathbf{Q}(\theta)$ be the chord of the Cornu spiral (1) from $\mathbf{Q}(\theta)$ to $\mathbf{Q}(\theta+\delta)$, $\theta > 0$, $0 < \delta \leq 2\pi$. If $\mathbf{T}_1$ and $\mathbf{T}_2$ are the unit tangent vectors to (1) at $\mathbf{Q}(\theta)$ and $\mathbf{Q}(\theta+\delta)$ respectively, then $\delta = \phi_1 + \phi_2$ and $0 < \phi_1 < \phi_2 < \pi$ where ϕ_1 is the angle from $\mathbf{T}_1$ to $\mathbf{D}$ and ϕ_2 is the angle from $\mathbf{D}$ to $\mathbf{T}_2$ as illustrated in Fig. 1.*

Proof. The ordering $\phi_1 < \phi_2$ follows immediately from a theorem by Vogt [6] (page 49). The rest follows by simple geometry. □

The following corollary, due to Ostrowski [6] (page 52), provides a necessary and sufficient condition for the existence of a spiral segment of positive curvature to match given G^1 Hermite data.

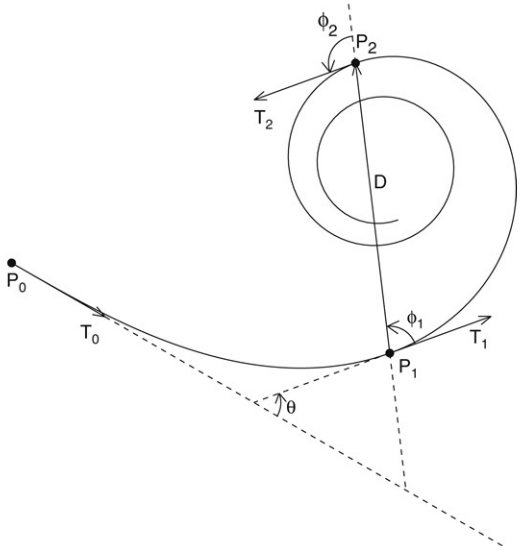

Fig. 1. C-shaped Cornu spiral chord.

Corollary 1. *Consider two points* $\mathbf{P}_1$, $\mathbf{P}_2$ *and corresponding unit tangent vectors* $\mathbf{T}_1$ *and* $\mathbf{T}_2$. *Let* $\phi_1 > 0$ *be the angle from* $\mathbf{T}_1$ *to* $\mathbf{D} = \mathbf{P}_2 - \mathbf{P}_1$ *and* $\phi_2 > 0$ *the angle from* $\mathbf{D}$ *to* $\mathbf{T}_2$. $\mathbf{P}_1$ *and* $\mathbf{P}_2$ *may be joined by a convex spiral arc with curvature increasing from* $\mathbf{P}_1$ *to* $\mathbf{P}_2$ *if and only if* $\phi_2 > \phi_1$.

Note that Corollary 1 does not guarantee that the spiral arc is a Cornu spiral segment. This is further explored in the section on a C-shaped Cornu spiral segment. If $\phi_1 > 0$, then a C-shaped segment is sought; if $\phi_1 \le 0$, or if a C-shaped segment does not exist for $\phi_1 > 0$, then an S-shaped segment is sought.

For convenience the function $h(\phi_1, \phi_2)$, which is used in subsequent proofs, is now defined as

$$h(\phi_1, \phi_2) = S(\phi_1 + \phi_2)\cos\phi_1 - C(\phi_1 + \phi_2)\sin\phi_1. \tag{3}$$

Note that $\phi_1 + \phi_2 > 0$ ensures that $S(\phi_1 + \phi_2), C(\phi_1 + \phi_2) > 0$.

Although Theorem 1 is used for the analysis of the C-shaped case and not for the S-shaped cases, it also aids in the decision of when the C-shaped formulation, or the S-shaped formulation, should be applied when the data are such that the beginning and ending tangent vectors point in directions which are on opposite sides of the chord joining the beginning and ending points.

4. A C-shaped Cornu spiral segment

Consider the point $\mathbf{P}_1$ on the Cornu spiral (1) for some $\theta \ge 0$, i.e. $\mathbf{Q}(\theta) = \mathbf{P}_1$. The angle from $\mathbf{T}_0$ to $\mathbf{D}$ is $\theta + \phi_1$. The tangent angle deviation from $\mathbf{P}_1$ to $\mathbf{P}_2$ is $\phi_1 + \phi_2$, hence $\mathbf{Q}(\theta + \phi_1 + \phi_2) = \mathbf{P}_2$ as shown in Fig. 1. Now from (1),

$$\begin{aligned} \mathbf{D} &= \mathbf{Q}(\theta + \phi_1 + \phi_2) - \mathbf{Q}(\theta) \\ &= a[C(\theta + \phi_1 + \phi_2) - C(\theta)]\mathbf{T}_0 + a[S(\theta + \phi_1 + \phi_2) - S(\theta)]\mathbf{N}_0. \end{aligned} \tag{4}$$

The dot products of (4) with $\mathbf{T}_0$ and $\mathbf{N}_0$ yield, after some algebraic manipulation, the following two equations in the two unknowns θ and a:

$$\|\mathbf{D}\| = a[S(\theta + \phi_1 + \phi_2) - S(\theta)]\sin(\theta + \phi_1) + a[C(\theta + \phi_1 + \phi_2) - C(\theta)]\cos(\theta + \phi_1) \tag{5}$$

and

$$f(\theta) = 0 \tag{6}$$

where

$$f(\theta) = \sqrt{2\pi}\{[S(\theta + \phi_1 + \phi_2) - S(\theta)]\cos(\theta + \phi_1) - [C(\theta + \phi_1 + \phi_2) - C(\theta)]\sin(\theta + \phi_1)\}. \tag{7}$$

Once (6) is solved for θ, a can be found directly from (5). By (2) and some trigonometric manipulation, (7) can be re-written as

$$f(\theta) = \int_{\theta}^{\theta+\phi_1+\phi_2} \frac{\sin(u-\theta-\phi_1)}{\sqrt{u}} \mathrm{d}u = \int_{-\phi_1}^{\phi_2} \frac{\sin u}{\sqrt{u+\theta+\phi_1}} \mathrm{d}u. \tag{8}$$

By Leibniz Rule for differentiation of a definite integral,

$$f'(\theta) = -\frac{1}{2}\int_{\theta}^{\theta+\phi_1+\phi_2} \frac{\sin(u-\theta-\phi_1)}{u^{3/2}} \mathrm{d}u = -\frac{1}{2}\int_{-\phi_1}^{\phi_2} \frac{\sin u}{(u+\theta+\phi_1)^{3/2}} \mathrm{d}u.$$

The following theorem determines when a unique C-shaped Cornu spiral segment, which matches the given G^1 Hermite data, can be found.

Theorem 2. *Let $0 < \phi_1 < \phi_2 < \pi$. If $h(\phi_1, \phi_2) > 0$ where $h(\phi_1, \phi_2)$ is defined by (3), then (6) has no solution for $\theta \geq 0$, and if $h(\phi_1, \phi_2) \leq 0$ then (6) has exactly one solution for $\theta \geq 0$; the solution occurs in the interval $[0, \theta_0]$ where*

$$\theta_0 = \frac{\lambda^2}{1-\lambda^2}(\phi_1+\phi_2) > 0 \tag{9}$$

and

$$0 < \lambda = \tfrac{1-\cos\phi_1}{1-\cos\phi_2} < 1 \tag{10}$$

as shown in Fig. 4 (b).

Proof. By introducing a change of integration variable, partitioning the interval of integration, and re-grouping, (8) can be re-written as

$$f(\theta) = \frac{1}{\sqrt{\theta+\phi_1}}[I_2(\theta) - I_1(\theta)] \tag{11}$$

where

$$I_1(\theta) = \int_0^{\phi_1} \frac{\sin u}{\left(1 - \frac{u}{\theta+\phi_1}\right)^{1/2}} \mathrm{d}u \tag{12}$$

and

$$I_2(\theta) = \int_0^{\phi_2} \frac{\sin u}{\left(1 + \frac{u}{\theta+\phi_1}\right)^{1/2}} \mathrm{d}u. \tag{13}$$

By differentiation,

$$I_1'(\theta) = -\frac{1}{2(\theta+\phi_1)^2}\int_0^{\phi_1} \frac{u \sin u}{\left(1 - \frac{u}{\theta+\phi_1}\right)^{3/2}} \mathrm{d}u$$

and

$$I_2'(\theta) = \frac{1}{2(\theta+\phi_1)^2}\int_0^{\phi_2} \frac{u \sin u}{\left(1 + \frac{u}{\theta+\phi_1}\right)^{3/2}} \mathrm{d}u.$$

It is clear that $I_1'(\theta) < 0$ and $I_2'(\theta) > 0$ on the interval $[0, \infty)$, so $I_1(\theta)$ is monotone decreasing, and $I_2(\theta)$ is monotone increasing on this interval. Furthermore, $\lim_{\theta\to\infty} I_1(\theta) = 1 - \cos\phi_1$ and $\lim_{\theta\to\infty} I_2(\theta) = 1 - \cos\phi_2$, hence $\lim_{\theta\to\infty} I_2(\theta) > \lim_{\theta\to\infty} I_1(\theta)$ for $0 < \phi_1 < \phi_2 < \pi$.

Observe that $f(0) = \sqrt{2\pi}\, h(\phi_1, \phi_2)$. So from (11), if $h(\phi_1, \phi_2) > 0$ then $I_2(0) > I_1(0)$, and if $h(\phi_1, \phi_2) \leq 0$ then $I_2(0) \leq I_1(0)$. It thus follows that if $h(\phi_1, \phi_2) > 0$ then $I_1(\theta)$ and $I_2(\theta)$ are never equal, in which case (6) does not have a solution, and if $h(\phi_1, \phi_2) \leq 0$ then they are equal exactly once, in which case (6) has exactly one solution, in $[0, \infty)$.

To establish that the solution (when $I_1(\theta)$ and $I_2(\theta)$ are equal exactly once) occurs in $[0, \theta_0]$, it remains to show that $I_2(\theta_0) \geq I_1(\theta_0)$. From (12) and (13)

$$I_1(\theta) \leq \int_0^{\phi_1} \frac{\sin u}{\left(1 - \frac{\phi_1}{\theta+\phi_1}\right)^{1/2}} \mathrm{d}u = \frac{1 - \cos\phi_1}{\left(1 - \frac{\phi_1}{\theta+\phi_1}\right)^{1/2}}$$

and

$$I_2(\theta) \geq \int_0^{\phi_2} \frac{\sin u}{\left(1 + \frac{\phi_2}{\theta+\phi_1}\right)^{1/2}} \mathrm{d}u = \frac{1 - \cos\phi_2}{\left(1 + \frac{\phi_2}{\theta+\phi_1}\right)^{1/2}}.$$

Hence

$$I_2(\theta_0) - I_1(\theta_0) \geq \frac{1 - \cos\phi_2}{\left(1 + \frac{\phi_2}{\theta_0+\phi_1}\right)^{1/2}} \left[1 - \frac{1 - \cos\phi_1}{1 - \cos\phi_2} \left(1 + \frac{\phi_1 + \phi_2}{\theta_0}\right)^{1/2}\right],$$

using θ_0 as given in (9) and (10), this becomes

$$I_2(\theta_0) - I_1(\theta_0) \geq 0. \quad \square$$

Corollary 2. *If* $\frac{1}{2}\pi \leq \phi_1 < \phi_2 < \pi$ *then* (6) *has exactly one solution in the interval* $[0, \theta_0]$.

Proof. It follows immediately since $h(\phi_1, \phi_2) < 0$ in this case. $\square$

Theorem 2 thus determines when a C-shaped segment of a Cornu spiral, that matches the given G^1 data described in Section 2.1, can be found. If it exists, then it is determined by finding the unique value of θ in the interval $[0, \theta_0]$ which satisfies Eq. (6); a bracketing method, e.g. Bolzano bisection, or Newton–Raphson's method combined with bracketing, can be used to find θ. Once θ is known, a is determined by (5), $\mathbf{T}_0$ is determined by rotating the unit vector $\mathbf{D}/\|\mathbf{D}\|$ an angle $\theta + \phi_1$ *clockwise* about $\mathbf{P}_1$. Eq. (1) then determines $\mathbf{P}_0$.

5. An S-shaped Cornu spiral segment

Let $\omega = -\theta$. Consider the point $\mathbf{P}_1$ on the Cornu spiral (1) for some $\omega > 0$, i.e. $-\mathbf{Q}(\omega) = \mathbf{P}_1$. The angle from $\mathbf{T}_0$ to $\mathbf{D}$ is $\omega + \phi_1$. The net change in the tangent angle from $\mathbf{P}_1$ to $\mathbf{P}_2$ is $\phi_1 + \phi_2$, hence $\mathbf{Q}(\omega + \phi_1 + \phi_2) = \mathbf{P}_2$ as shown in Fig. 2. Now from (1),

$$\begin{aligned} \mathbf{D} &= \mathbf{Q}(\omega + \phi_1 + \phi_2) - \mathbf{Q}(\omega) \\ &= a[C(\omega + \phi_1 + \phi_2) + C(\omega)]\mathbf{T}_0 + a[S(\omega + \phi_1 + \phi_2) + S(\omega)]\mathbf{N}_0. \end{aligned} \tag{14}$$

The dot products of (14) with $\mathbf{T}_0$ and $\mathbf{N}_0$ yield, after some algebraic manipulation, the following two equations in the two unknowns ω and a:

$$\|\mathbf{D}\| = a[S(\omega + \phi_1 + \phi_2) + S(\omega)]\sin(\omega + \phi_1) + a[C(\omega + \phi_1 + \phi_2) + C(\omega)]\cos(\omega + \phi_1) \tag{15}$$

and

$$g(\omega) = 0 \tag{16}$$

where

$$\begin{aligned} g(\omega) &= \sqrt{2\pi}\{[S(\omega + \phi_1 + \phi_2) + S(\omega)]\cos(\omega + \phi_1) - [C(\omega + \phi_1 + \phi_2) + C(\omega)]\sin(\omega + \phi_1)\} \qquad (17) \\ &= \int_0^{\omega+\phi_1+\phi_2} \frac{\sin(u - \omega - \phi_1)}{\sqrt{u}} \mathrm{d}u + \int_0^{\omega} \frac{\sin(u - \omega - \phi_1)}{\sqrt{u}} \mathrm{d}u, \qquad (18) \end{aligned}$$

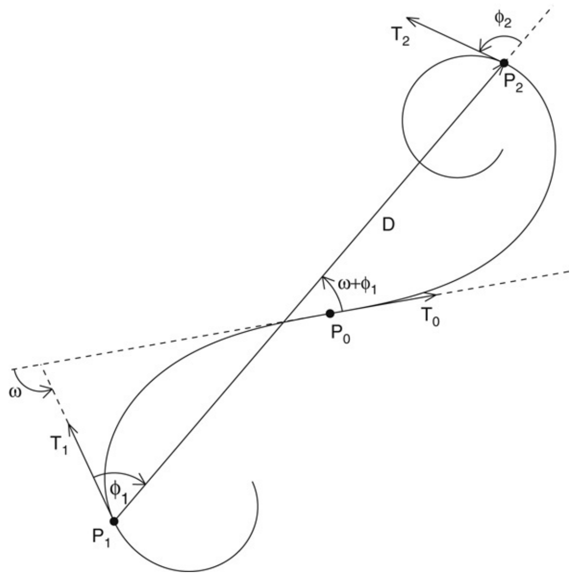

Fig. 2. S-shaped Cornu spiral chord.

or, by introducing a change of integration variable, partitioning the interval of integration, and re-grouping,

$$g(\omega) = 2\int_0^{\omega+\phi_1} \frac{\sin(u-\omega-\phi_1)}{\sqrt{u}}\mathrm{d}u + \int_0^{\phi_2} \frac{\sin u}{\sqrt{\omega+\phi_1+u}}\mathrm{d}u + \int_0^{\phi_1} \frac{\sin u}{\sqrt{\omega+\phi_1-u}}\mathrm{d}u. \tag{19}$$

Applying Leibniz rule for differentiation of a definite integral to (19) yields

$$g'(\omega) = -2\int_0^{\omega+\phi_1} \frac{\cos(u-\omega-\phi_1)}{\sqrt{u}}\mathrm{d}u - \frac{1}{2}\int_0^{\phi_2} \frac{\sin u}{(\omega+\phi_1+u)^{3/2}}\mathrm{d}u - \frac{1}{2}\int_0^{\phi_1} \frac{\sin u}{(\omega+\phi_1-u)^{3/2}}\mathrm{d}u. \tag{20}$$

There are two cases to be considered for the S-shaped segment:

- $0 < \phi_1 < \phi_2 < \pi$, $h(\phi_1, \phi_2) > 0$ where $h(\phi_1, \phi_2)$ is defined by (3), and
- $-\pi < \phi_1 \le 0 < \phi_2 \le \pi$.

The following two theorems show that a unique S-shaped Cornu spiral segment, which matches the given G^1 Hermite data, can always be found in each of the above two cases.

Theorem 3. *Let $0 < \phi_1 < \phi_2 < \pi$. If $h(\phi_1, \phi_2) > 0$ where $h(\phi_1, \phi_2)$ is defined by (3), then (16) has exactly one solution in the interval* $[0, \frac{1}{2}\pi - \phi_1]$.

Proof. It follows from (3) that $h(\phi_1, \phi_2) \le 0$ for $\frac{1}{2}\pi \le \phi_1 < \pi$, so $0 < \phi_1 < \frac{1}{2}\pi$. All the integrals in (20) are positive for $0 \le \omega + \phi_1 \le \frac{1}{2}\pi$, so $g(\omega)$ is monotone decreasing on $[0, \frac{1}{2}\pi - \phi_1]$. Furthermore, from (17), $g(0) = \sqrt{2\pi}h(\phi_1, \phi_2) > 0$ and $g(\frac{1}{2}\pi - \phi_1) < 0$. Hence, $g(\omega)$ decreases monotonically from a positive value to a negative value on the interval $[0, \frac{1}{2}\pi - \phi_1]$. □

Theorem 4. *If $-\pi < \phi_1 \le 0 < \phi_2 \le \pi$, then (16) has exactly one solution for $0 \le \omega \le \frac{1}{2}\pi - \phi_1$. The solution occurs in the interval* $[-\phi_1, \frac{1}{2}\pi - \phi_1]$.

Proof. By a change of integration variable, the third integral of (20) is

$$\int_0^{\phi_1} \frac{\sin u}{(\omega+\phi_1-u)^{3/2}}\mathrm{d}u = \int_0^{-\phi_1} \frac{\sin u}{(\omega+\phi_1+u)^{3/2}}\mathrm{d}u \ge 0.$$

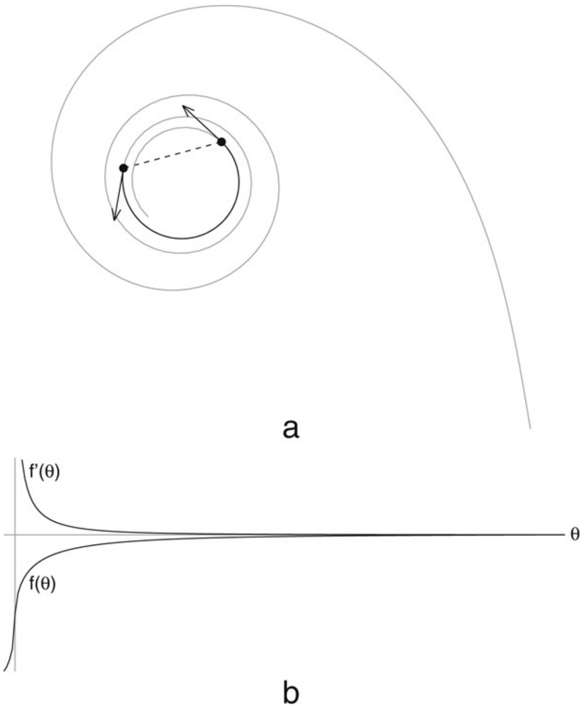

Fig. 3. Example 1. $\phi_1 = 115°, \phi_2 = 122°$.

It thus follows that $g'(\omega) \le 0$ for $\omega \in [-\phi_1, \frac{1}{2}\pi - \phi_1]$. Furthermore, from (17), $g(-\phi_1) > 0$ and $g(\frac{1}{2}\pi - \phi_1) < 0$. Hence, $g(\omega)$ decreases monotonically from a positive value to a negative value on the interval $[-\phi_1, \frac{1}{2}\pi - \phi_1]$. It remains to show that $g(\omega) > 0$ on the interval $[0, -\phi_1]$.

Observe that if $0 \le \omega \le -\phi_1$ and $-\pi \le \phi_1 \le 0$, then $-\pi \le \phi_1 \le \omega + \phi_1 \le 0$. Consider now the integrands and integration intervals for (18). For the first integral

$$0 \le -\omega - \phi_1 \le u - \omega - \phi_1 \le \phi_2 < \pi,$$

and for the second integral

$$0 \le -\omega - \phi_1 \le u - \omega - \phi_1 \le -\phi_1 < \pi.$$

Hence $g(\omega) > 0$ on the interval $[0, -\phi_1]$. □

If a C-shaped segment of a Cornu spiral does not match the given G^1 data described in Section 2.1, then an S-shaped Cornu spiral segment does. It is determined by finding the unique value of ω in the interval $(\max(0, -\phi_1), \frac{1}{2}\pi - \phi_1)$, which satisfies Eq. (16); a bracketing method, e.g. Bolzano bisection, or Newton–Raphson's method combined with bracketing, can be used to find ω. Now a is determined by (15), $\mathbf{T}_0$ is determined by rotating the unit vector $\mathbf{D}/\|\mathbf{D}\|$ an angle $\omega + \phi_1$ *clockwise* about $\mathbf{P}_1$, and $\theta = -\omega$, so $\mathbf{P}_0$ is determined by Eq. (1).

6. Examples

The methods described above were implemented in Java and tested on many examples of which the five listed below are representative. The G^1 Hermite data for the examples are shown graphically as dots and arrows in Figs. 3(a), 4(a), 5(a), 6(a) and 7(a). The interpolating Cornu spiral segments are drawn with solid black lines. Gray lines are used to illustrate extensions of the Cornu spiral, including its inflection point, to its interpolating segment. Plots of the relevant parts of the functions $f(\theta)$ and $g(\omega)$ as well as their derivatives are shown in Figs. 3(b), 4(b), 5(b), 6(b) and 7(b).

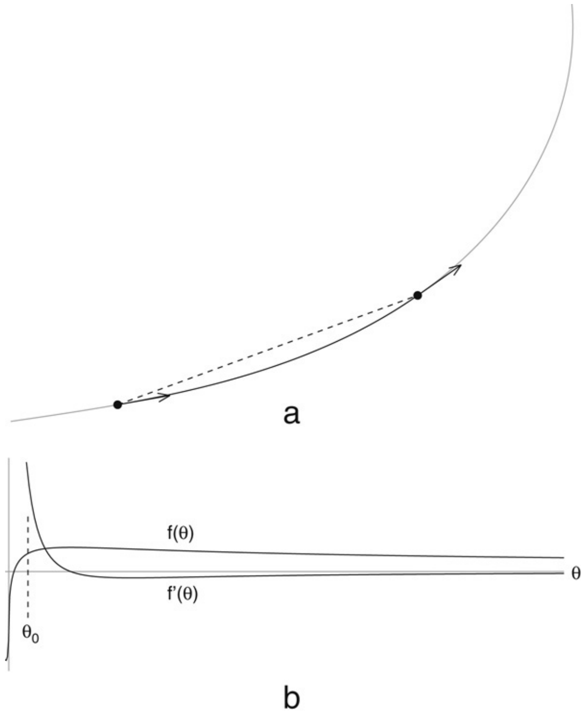

Fig. 4. Example 2. $\phi_1 = 10^\circ, \phi_2 = 15^\circ$.

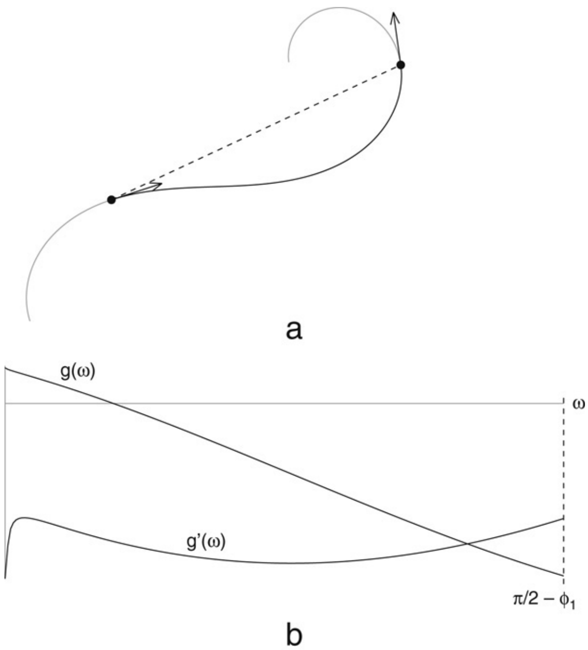

Fig. 5. Example 3. $\phi_1 = 7^\circ, \phi_2 = 73^\circ$.

6.1. Example 1

For this example, $\phi_1 = 115^\circ$ and $\phi_2 = 122^\circ$. It illustrates a solution to (6) for a value of $\theta \approx 4.9\pi > 2\pi$.

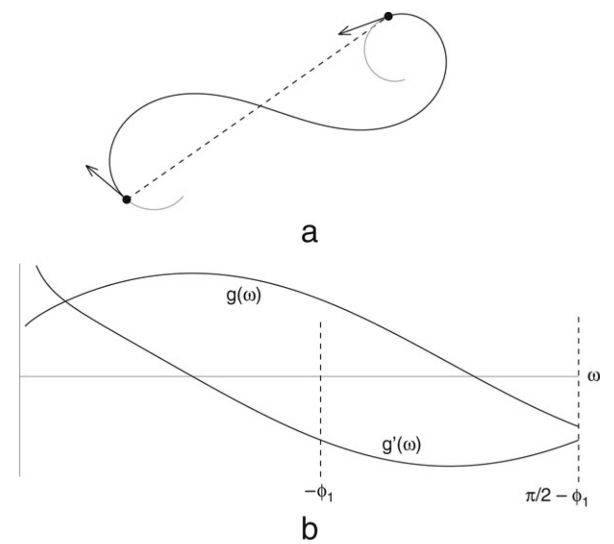

Fig. 6. Example 4. $\phi_1 = -105°$, $\phi_2 = 165°$.

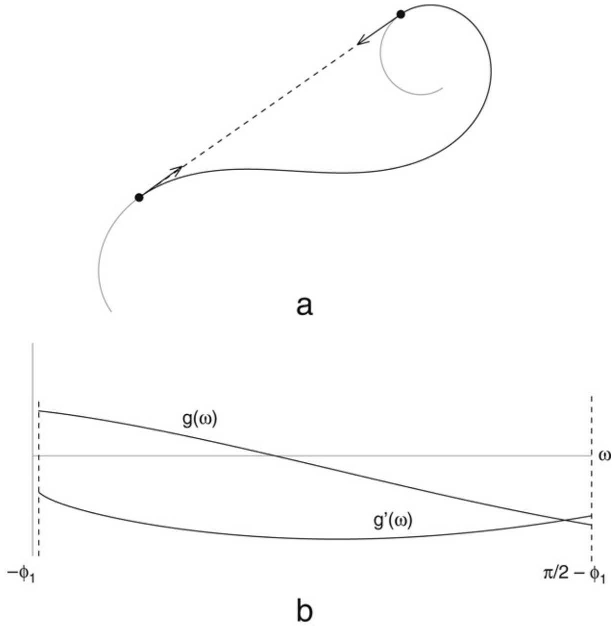

Fig. 7. Example 5. $\phi_1 = -1°$, $\phi_2 = 180°$.

6.2. Example 2

For this example, $\phi_1 = 10°$ and $\phi_2 = 15°$. It illustrates a solution to (6) for a value of $\theta \approx 0.009\pi$.

6.3. Example 3

For this example, $\phi_1 = 7°$ and $\phi_2 = 73°$. It illustrates an S-shaped solution when a C-shaped solution does not exist for both ϕ_1 and ϕ_2 greater than zero.

6.4. Example 4

For this example, $\phi_1 = -105°$ and $\phi_2 = 165°$. It illustrates an S-shaped solution for $\phi_1 < 0$ and $\phi_2 > 0$.

6.5. Example 5

For this example, $\phi_1 = -1°$ and $\phi_2 = 180°$. It illustrates an S-shaped solution for which the net change in the tangent angle is 179°. The net change in the other two S-shaped examples is smaller than 90°.

7. Conclusion

The new proposed method is based on simple bisection or Newton–Raphson iteration which is simpler than numerical optimization. The problem is formulated and solved as a G^1 Hermite interpolation problem for a Cornu spiral segment without pre-processing. Unlike a biarc, the Cornu spiral segment naturally has exactly the correct number of degrees of freedom for the G^1 match, so the solution need not be constrained. The solution is guaranteed. For the C-shaped case the solution is unique. For the S-shaped case, an interval arises naturally which guarantees that the angle of tangent deviation will not exceed 2π. It is thus not necessary to consider a critical constraint to assure this, as is done for the biarc fit in [8].

It can be observed that the G^1 data are naturally partitioned into three mutually exclusive sets, namely

- $0 < \phi_1 < \phi_2 < \pi, h(\phi_1, \phi_2) \leq 0$,
- $0 < \phi_1 < \phi_2 < \pi, h(\phi_1, \phi_2) > 0$, and
- $-\pi < -\phi_2 < \phi_1 \leq 0 \leq \phi_2 \leq \pi$.

The first set gives rise to a C-shaped segment, whereas the other two sets give rise to S-shaped segments.

The method is a suitable alternative for any problem in which biarcs are typically used, e.g. filling in gaps of spiral curves [13], and toolpaths for CNC machining [20]. In the latter reference, biarcs were used to accommodate machines whose controllers only allowed toolpaths consisting of straight line segments and circular arcs. However, there is currently progress which will enable spiral arcs to be used in CNC machine toolpaths [14,10].

Acknowledgements

The authors acknowledge with thanks the suggestions of the anonymous reviewer which helped to improve the paper. The authors were supported by the Natural Sciences and Engineering Research Council of Canada.

References

[1] M. Abramowitz, I.A. Stegun, Handbook of Mathematical Functions, Dover Publications, Inc., New York, 1977.
[2] K.G. Baass, The use of clothoid templates in highway design, Transportation Forum 1 (1984) 47–52.
[3] E. Degtiariova-Kostova, V. Kostov, Irregularity of optimal trajectories in a control problem for a car-like robot, INRIA Sophia Antipolis Research Report 3411, France, April 1998.
[4] R.T. Farouki, C. Manni, A. Sestini, Shape-preserving interpolation by G^1 and G^2 PH quintic splines, IMA Journal of Numerical Analysis 23 (2003) 175–195.
[5] S. Fleury, P. Souéres, J.-P. Laumond, R. Chatila, Primitives for smoothing mobile robot trajectories, in: Proc. IEEE International Conference on Robotics and Automation, 1993, pp. 832–839.
[6] H.W. Guggenheimer, Differential Geometry, Dover Publications, Inc., New York, 1977.
[7] T.F. Hickerson, Route Location and Design, McGraw-Hill, New York, 1964.
[8] B.B. Kimia, I. Frankel, A.-M. Popescu, Euler spiral for shape completion, International Journal of Computer Vision 54 (1–2–3) (2003) 159–182.
[9] D.E. Knuth, Mathematical typography, Bulletin (new series) of the American Mathematical Society 1 (2) (1979) 337–372.
[10] H. Makino, Clothoidal interpolation — a new tool for high-speed continuous path control, Annals of the CIRP 37 (1) (1988) 25–28.
[11] D.S. Meek, D.J. Walton, The use of Cornu spirals in drawing planar curves of controlled curvature, Journal of Computational and Applied Mathematics 25 (1989) 69–78.
[12] D.S. Meek, D.J. Walton, Clothoid spline transition spirals, Mathematics of Computation 59 (199) (1992) 117–133.
[13] D.S. Meek, D.J. Walton, The family of biarcs that matches planar, two-point G^1 Hermite data, Journal of Computational and Applied Mathematics 212 (1) (2008) 31–45.
[14] A.P. Pamali, Using clothoidal spirals to generate smooth tool paths for high speed machining, M.Sc. Thesis, North Carolina State University, 2004.
[15] A. Scheuer, Th. Fraichard, Continuous-curvature path planning for car-like vehicles, in: Proc. IEEE Int. Conf. Intelligent Robots and Systems, vol. 2, 1997. pp. 997–1003.
[16] S. Ullman, Filling-in the gaps: The shape of subjective contours and a model for their generation, Biological Cybernetics 25 (2) (1976) 1–6.
[17] D.J. Walton, D.S. Meek, Computer-aided design for horizontal alignment, ASCE Journal of Transportation Engineering 115 (4) (1989) 411–424.
[18] D.J. Walton, D.S. Meek, Clothoidal splines, Computers & Graphics 14 (1) (1990) 95–100.
[19] D.J. Walton, D.S. Meek, A controlled clothoid spline, Computers & Graphics 29 (2005) 353–363.
[20] M.K. Yeung, D.J. Walton, Curve fitting with arc splines for NC tool path generation, Computer-Aided Design 26 (11) (1994) 845–849.